Vanishing order-parameter critical fluctuations of an absorbing-state transition driven by long-range interactions

C. Argolo,[1,2] Yan Quintino,[1] Pedro H. Barros,[1] and M. L. Lyra[2,*]

[1]*Instituto Federal de Ciência e Tecnologia do Estado de Alagoas, 57020-510 Maceió-AL, Brazil*

[2]*Instituto de Física, Universidade Federal de Alagoas, 57072-970 Maceió AL, Brazil*

(Received 29 November 2012; revised manuscript received 19 February 2013; published 19 March 2013)

We study the critical behavior of the absorbing-state phase transition depicted by a contact process one-dimensional model system with power-law decaying interactions. The system dynamical processes include particle creation at a rate which decays with the distance from the nearest particle as $1/r^{\alpha}$. This model displays an absorbing-state phase transition with critical exponents varying continuously with the interaction exponent α. Here, we provide a finite-size scaling analysis of the stationary order-parameter density, one of its moment ratio, its logarithmic derivative, and fluctuations. We also follow the short-time relaxation dynamic of these quantities to estimate their corresponding dynamical critical exponents. The estimated exponents are shown to be consistent with the hyperscaling relation. Further, we report an unconventional regime on which the critical order-parameter fluctuations vanish in the thermodynamic limit.

DOI: 10.1103/PhysRevE.87.032141 PACS number(s): 05.70.Jk, 64.60.Ht, 05.50.+q, 64.60.De

I. INTRODUCTION

The fluctuation dissipation theorem [1] is an important tool in statistical physics that shows a direct relation between the response of a system in thermal equilibrium to an external stimulus and its spontaneous fluctuations. The most widely known relations are that between the heat capacity of a system and its energy fluctuations as well as the susceptibility to an external field and the order-parameter fluctuations. The diverging susceptibility at an equilibrium second-order transition thus leads to diverging fluctuations, as observed through the phenomenon of critical opalescence occurring at the critical point presented by ordinary substances at the end of the first-order liquid-gas transition line. However, nonequilibrium phase transitions from an active to an absorbing state have been a topic of large interest in this field [2–7]. In this class of systems, there is no detailed balance and the fluctuation-dissipation theorem does not hold, features that are usually explored in studies of equilibrium phase transitions. In particular, the behavior of the susceptibility and order-parameter fluctuations in the vicinity of the transition are governed by distinct critical exponents [8,9].

A simple example of a model presenting a dynamic transition into absorbing states is the contact process (CP) [10]. It is a model that shows competition between two elementary processes in a spatially distributed population. Self-replication is permitted and also spontaneous annihilation of the components. An example is a Markov process in which each site of a lattice presents two possible states, named *active* and *inactive*. A short lifetime of active sites results in the whole system being driven to the absorbing state with only inactive sites. Above a critical lifetime, the system reaches a stationary active state with a fluctuating finite fraction of active sites which is the proper order parameter [5–7]. The universality class of the CP is the directed percolation (DP) class. The DP universality class has been observed to describe a large class of models presenting a dynamic transition into a single absorbing state [2]. Recently, this universality class was experimentally shown to govern the phase transition between two topologically different turbulent states of electrohydrodynamic convection in nematic liquid crystals [11,12]. In the mean-field regime, the order-parameter fluctuations develop just a discontinuity at the critical point, thus implying a vanishing critical exponent. In the contact process, a spontaneous generation rate acts as the conjugated field and the susceptibility diverges as the critical point is approached [8,9]. The standard set of mean-field exponents are $\beta = \nu_{\parallel} = 1$, $\nu_{\perp} = 1/2$, $\gamma = 1$, and $\gamma' = 0$, where β is the order-parameter critical exponent, $\nu_{\parallel}$ stands for the correlation time critical exponent, $\nu_{\perp}$ is the correlation length exponent, γ is the susceptibility exponent, and γ' corresponds to the exponent governing the order-parameter critical fluctuations. In low dimensions, the mean-field theory does not apply and the exponents depict significant corrections. For example, accurate estimates for the critical exponents for the one-dimensional contact process read $\beta = 0.276$, $\nu_{\parallel} = 1.734$, $\nu_{\perp} = 1.097$, $\gamma = 2.778$, and $\gamma' = 0.544$ [8].

In spite of the robustness of the DP, examples of models not belonging to the universality class of directed percolation exist and some are firmly established, as, for example, in parity-conserving processes in branching and annihilation random walks [13], the voter universality class appearing in the model of an order-disorder transition with a Z_2 symmetry driven by interfacial noise [14], an absorbing-state phase transition with a conserved field [15], absorbing-state transitions in the presence of particle diffusion [16–25], the diffusive pair contact process [26], and epidemic processes with long-range interactions [27–32], among others [2–4]. The presence of long-range interactions usually implies in a set of critical exponents that continuously depend on the range of the interactions in nonequilibrium [27–32] as well as in equilibrium phase transitions [33–36].

Here we will focus on the critical behavior of the long-range epidemic process, where inactive sites can be activated over long distances introduced by Ginelli *et al.* [30]. The evolution of the model is made by a random sequential updating of the

*marcelo@df.ufal.br

states of sites located in a linear closed chain. Each site can be in an active state (referred as state 1) or in an inactive state (referred as state 0). These states undergo the following reactions:

$$1 \to 0 \quad \text{with rate } 1, \tag{1}$$

$$0 \to 1 \quad \text{with rate } \lambda/r^{\alpha}, \tag{2}$$

where λ is the first-neighbors infection rate and r is the distance to the nearest active site. The presence of a long-range activation process is an important mechanism that can influence the critical behavior of systems with absorbing states. Usually, active and inactive sites mimic healthy and sick individuals. On long distances, sick individuals may infect healthy ones at a rate λ/r^{α}. They also recover spontaneously at a unitary rate. Therefore, a competition between the contamination process (creation of active sites) and the recovery process (annihilation of active) takes place. For low infection rates, the stationary state is characterized by a global extinction of the epidemics. Above a critical infection rate $\lambda_c(\alpha)$ there is a stable steady-state regime with a fluctuating finite density of sick individuals (active sites). Near $\lambda_c(\alpha)$ the system exhibits a phase transition with the average density of sick individuals acting as the order parameter. The model has some connection with studies of depinning transitions in nonequilibrium wetting processes because the restricted long-range contact process presents an analogy with the depinning process [30,31].

Above the critical dimension $d_c = 4$ fluctuations in the particle densities are irrelevant and the system is well described by a mean-field approach. For lower dimensions, corrections to the mean-field picture must be considered [5]. The particular case of $\alpha \to \infty$ recovers the short-range dynamics of the standard contact process. For $\alpha < 1$ the system remains in the active state for any finite value of the contamination rate λ. Within a mean-field approach and by numerical simulations in linear chains, it has been shown that the critical exponents vary continuously as α decreases, i.e., when the activation process becomes more long ranged. A proper mean-field approximation for the one-dimensional long-ranged epidemic process predicts $\nu_\perp = \beta = 1/(\alpha - 1)$ and $\nu_\parallel = 1$ for $1 < \alpha < 2$. In the intermediate regime of $2 < \alpha < 3$ it provides $\nu_\perp = 2 - \alpha/2$ and $\beta = \nu_\parallel = 1$, while standard mean-field exponents for the directed percolation universality class in systems with short-range interactions $\nu_\perp = 1/2$ and $\beta = \nu_\parallel = 1$ hold for $\alpha > 3$. Considering the short-time relaxation process of the order parameter at the critical point, a couple of critical exponents were numerically estimated [30]. While being distinct from the mean-field prediction in all ranges of the interaction exponent α, these followed the predicted trend, in particular, the continuous variation of the exponents with α and the divergence of the order-parameter exponent β as $\alpha \to 1$. Nonequilibrium phase transitions characterized by an order-parameter exponent β above the unit are quite rare and may exhibit features not shared by conventional second-order phase transitions.

In the present work, we advance the study of the critical behavior presented by the long-range epidemic process (LREP). First, we will study the critical behavior in the stationary regime. We will show that a finite-size scaling analysis of the order-parameter moment ratio can be used to identify the critical point, although strong corrections to scaling develop as α decreases. The size dependence of the order parameter, its logarithmic derivative, and fluctuations at the critical point are used to estimate three stationary critical exponents. A short-time dynamics study is also provided to obtain the corresponding dynamical exponents of these quantities. In particular, we will unveil an unconventional regime at which the critical order-parameter fluctuations vanish as the system size increases.

The manuscript is organized as follows: In Sec. II we present the model and describe the main aspects of the numerical simulation. In Sec. III, we present our results for the critical behavior based on the finite-size scaling of data obtained from simulations in linear chains in the stationary state. In Sec. III, we also report a short time dynamics study of the critical behavior. Finally, we summarize and discuss our main results in Sec. IV.

II. MODEL AND SIMULATION DETAILS

In what follows, we consider a stochastic dynamical process taking place at a population of individuals that can be either in an inactive (uninfected state 0) or in an active (infected state 1) state. These individuals occupy all sites of a one-dimensional closed chain and are not allowed to diffuse. Sites in the active state have a finite lifetime, becoming inactive at a unitary rate. Inactive sites can be activated through a long-distance interaction with the nearest neighbor active individual, obeying the infection rule described by Eq. (2) that assumes an activation rate λ/r^{α}, with r being the distance to the nearest active site. Numerically, for the purpose of Monte Carlo simulations, sites are chosen at random. Whenever the chosen site is active, it is deactivated with a probability $1/(1 + \lambda)$. On the other hand, an inactive site is activated with probability $(\lambda/r^{\alpha})/(1 + \lambda)$.

The competition between the contamination process and the recovery process leads to a transition between an inactive global state at low infection rates and a stable active state with a fluctuating density of active sites at high contamination rates. The presence of a long-range process can influence the critical behavior of systems with absorbing states. This fact makes long-range epidemic process an interesting model to study [30], as deviations from the DP class can be observed. For small values of α, the critical infection rate for the spreading of the epidemic is low and one expects the long-range activation to be the main mechanism responsible for the propagation of the disease. Increasing α will bring the system to a pure CP process, since, in this case, the activation process is effectively driven by the nearest-neighbors sites. In this sense, the transition in this regime shall present features similar to the usual DP transition.

In our simulations, we considered chains with L sites and periodic boundary conditions. At each lattice sweep (considered as the time unit), we performed the update of L sites chosen according to a random sequence. In this way, the same site can be eventually updated more than once in a given lattice sweep while others may remain unaffected. Since any finite system eventually becomes trapped in the vacuum state, we activated an individual chosen at random whenever the system becomes trapped, i.e., we assumed the vacuum state as a reflective boundary. This approach has been successfully

used in the literature and it is able to accurately account for the critical behavior of the absorbing-state phase transition after a proper finite-size scaling analysis. In order to identify the transition between the vacuum and steady active state, we considered the stationary density of active sites as the order parameter $\Psi(\lambda, L) = \langle N_a(\lambda, L)\rangle / L$, where $\langle N_a\rangle$ is the average number of active sites in the statistically stationary regime. Therefore, after starting with a random distribution of active and inactive sites, we disregard the initial L^2 lattice sweeps in order to reach the statistically stationary regime and performed the average of the density of active sites over 10^4 distinct uncorrelated configurations taken at each L lattice sweeps.

III. RESULTS

The order parameter in the vicinity of the critical activation rate λ_c for two representative values of the exponent α governing the range of the long-range interaction is shown in Fig. 1. Here we considered the estimates for the critical point reported in Ref. [30]. One can notice a striking difference between the two cases. For $\alpha = 3.0$, the order-parameter density has the usual sigmoid form in the vicinity of the critical point, which becomes more pronounced as the system size increases, thus signaling its diverging derivative in the thermodynamic limit as the transition is approached from the active side. On the other hand, the order-parameter density is much smoother in the vicinity of the transition for $\alpha = 1.5$. These data point towards a vanishing derivative of the critical point. This feature is in agreement with the mean-field prediction and the numerical simulations [30] of an order-parameter exponent $\beta > 1$ for low values of α.

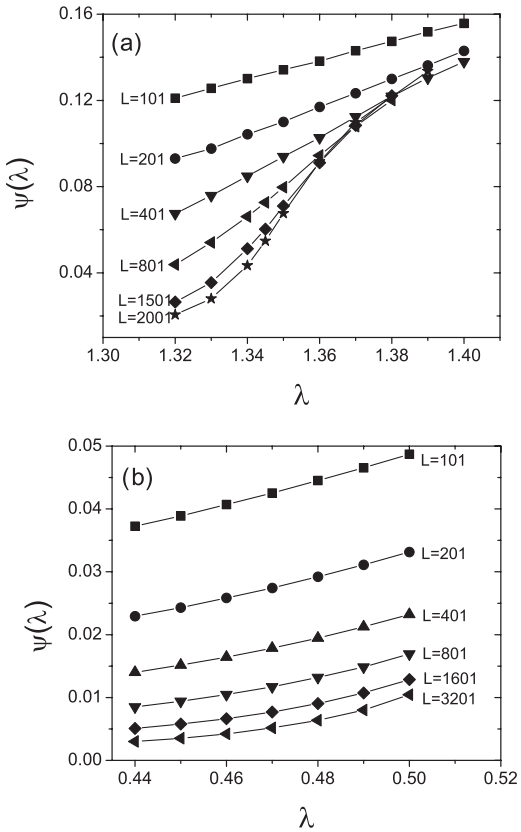

FIG. 1. Average stationary density of individuals in the active state in the vicinity of the transition versus the infection rate λ for distinct lattice sizes. The stationary regime was considered to be achieved after L^2 lattice sweeps. The average was performed considering 10^4 distinct configurations taken at each L lattice sweeps. Data were obtained from simulations with $\alpha = 3$ (a) and $\alpha = 1.5$ (b).

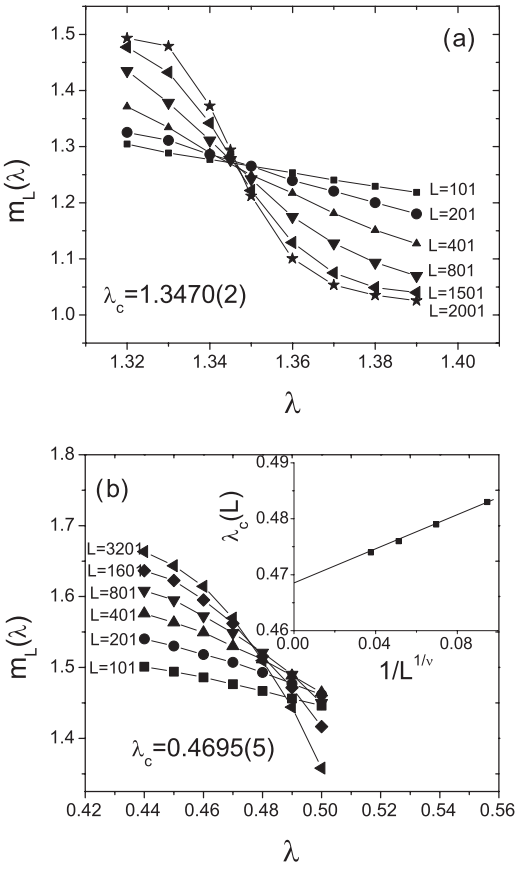

FIG. 2. (a) The moment ratio $m_L(\lambda)$ as a function of the infection rate λ for distinct lattice sizes and $\alpha = 3$. The scale invariance at the critical point provides a precise estimate of the critical infection rate λ_c. (b) Same calculations for $\alpha = 1.5$. For such a long-range contamination process, there are large corrections to scaling. A finite-size scaling analysis of the crossing points (shown in the inset) provides the best estimate of the critical contamination rate in the limit of $L \to \infty$.

In order to confirm the accuracy of the critical points reported in Ref. [30], we computed the stationary order-parameter moment ratio defined as $m_L(\lambda) = \langle N_a^2\rangle / \langle N_a\rangle^2$. When considering data from distinct system sizes, this moment ratio is known to be scale invariant at the absorbing-state phase transition in the regime of large sizes [9,37]. In Fig. 2 we report data for the above order-parameter moment ratio for the same two values of α used in Fig. 1. For $\alpha = 3.0$ the data show a quite well-defined crossing point signaling the scale invariance at the transition. The scale-invariant point is in excellent agreement with the critical point reported in Ref. [30] [shown as a legend in Fig. 2(a)]. For $\alpha = 1.5$ the crossings of data from distinct sizes are spread over a small, but significant, region [see Fig. 2(b)]. This feature indicates that corrections to scaling become more pronounced as the activation process becomes longer ranged. However, the finite-size scaling plot

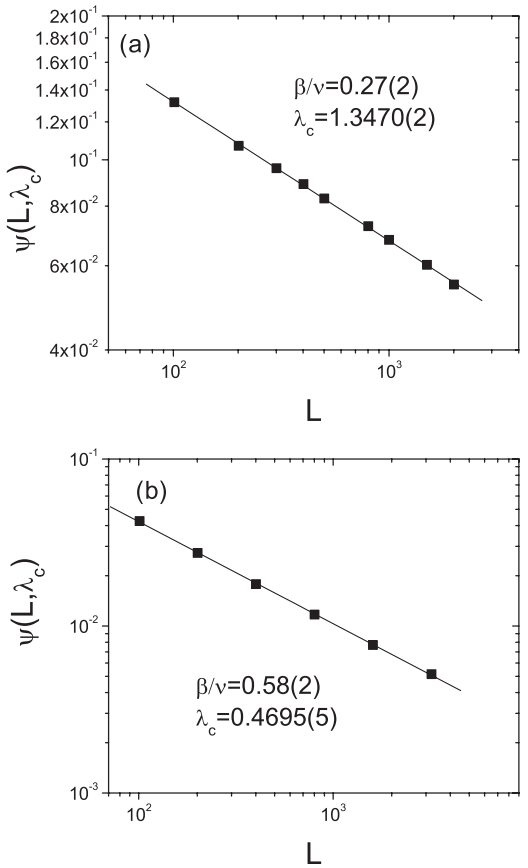

FIG. 3. (a) Finite-size scaling of the order parameter at the critical point $\lambda_c = 1.3470(2)$ for $\alpha = 3$. From the best fit to a power law, we estimate the critical exponent ratio $\beta/\nu_\perp = 0.27(2)$. The error bar includes the error in the estimate of the critical density. (b) The same for $\alpha = 1.5$. In this case, the critical contamination rate is $\lambda_c = 0.4695(5)$ and our best estimate provided $\beta/\nu_\perp = 0.58(2)$.

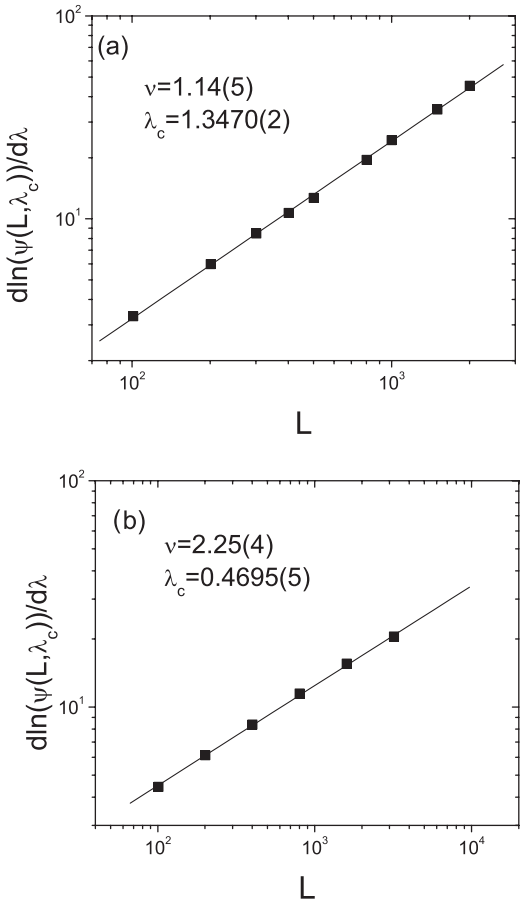

FIG. 4. Finite-size scaling of the logarithmic derivative of the order parameter at the critical point. From the best fit to power laws, we estimated the correlation length critical exponent $\nu_\perp$. For $\alpha = 3.0$ (a) we obtained $\nu = 1.14(5)$ while $\nu_\perp = 2.25(4)$ for $\alpha = 1.5$ (b).

of the crossing points reported as an inset in Fig. 2(b) allows us to infer the location of the critical point in the thermodynamic limit. Once again, the agreement with the estimate of Ref. [30] is excellent. In what follows, we will employ a finite-size and finite-time scaling analysis of the critical behavior for several values of α using the set of critical activation rates reported in such previous study.

We begin by exploring the finite-size scaling behavior of the statistically stationary order-parameter density at the critical point. According to the single length scale hypothesis, the order parameter at the critical point shall scale with the system size as $\Psi(\lambda_c, L) \propto L^{-\beta/\nu_\perp}$, where β and $\nu_\perp$ are the order parameter and correlation length critical exponents, respectively. Further, the derivative of the order-parameter density at the critical point can be used to give an independent estimate for $\nu_\perp$. Based in the scaling hypothesis that in the vicinity of the critical point the order-parameter density can be put in the form

$$\Psi(\lambda, L) = L^{-\beta/\nu_\perp} f[L^{1/\nu_\perp}(\lambda - \lambda_c)], \tag{3}$$

it can be easily verified that the logarithmic derivative of the order-parameter density at the critical point shall scale as $\partial[\ln \Psi(\lambda, L)]/\partial\lambda|_{\lambda_c} \propto L^{1/\nu_\perp}$. We illustrate the finite-size scaling behavior of the order parameter and its logarithmic derivative at the critical point in Figs. 3 and 4, respectively, using the same representative values of the exponent α used in the previous figures. Both quantities follow very precisely the scaling hypothesis, even for small values of α. The set of estimated critical exponents are summarized in Table I.

The reported values of the critical exponent ratio $\beta/\nu_\perp$ suggest that a nonconventional critical behavior develops at

TABLE I. Estimated stationary critical exponents $\beta/\nu_\perp$, $1/\nu_\perp$, and $\gamma'/\nu_\perp$ for various values of the exponent α characterizing the long-distance infection process. The critical infection rate λ_c were taken from Ref. [30]. Note that the critical exponent governing the critical fluctuations of the order parameter γ' is negative for $\alpha \gtrsim 1.7$, thus indicating a regime of vanishing critical fluctuations. The predicted values of $(2\beta + \gamma')/\nu_\perp$ are also included and shown to satisfy the hyperscaling relation.

α	λ_c	$\beta/\nu_\perp$	$\nu_\perp$	$\gamma'/\nu_\perp$	$(2\beta+\gamma')/\nu_\perp$
1.2	0.205(3)	0.80(5)	3.47(3)	−0.51(5)	1.09(15)
1.5	0.4695(5)	0.58(2)	2.25(4)	−0.17(2)	0.99(6)
1.8	0.714(1)	0.46(3)	1.73(2)	0.10(2)	1.02(8)
2.0	0.8592(2)	0.39(5)	1.51(2)	0.23(6)	1.01(16)
2.5	1.1492(2)	0.30(3)	1.42(3)	0.41(6)	1.01(12)
3.0	1.3470(2)	0.27(2)	1.14(5)	0.44(2)	0.98(6)

small values of α. According to the hyperscaling hypothesis, the order parameter, correlation length, and order-parameter fluctuation critical exponents shall obey the relation $2\beta + \gamma' = d\nu_\perp$, where d is the system dimensionality. The order-parameter fluctuations are defined as

$$\Delta\Psi = \left(\langle N_a^2\rangle - \langle N_a\rangle^2\right)L, \tag{4}$$

which, in the vicinity of the critical point, scales as $\delta\Psi \propto (\lambda - \lambda_c)^{-\gamma'}$. In finite systems, the order-parameter fluctuations at the critical point shall scale as $\Delta\Psi_L(\lambda_c) \propto L^{\gamma'/\nu_\perp}$. In equilibrium phase transitions, the order-parameter fluctuations are directly related to the susceptibility to an external ordering field according to the fluctuation-dissipation theorem. The divergence of the system susceptibility at a second-order phase transition thus implies divergent order-parameter critical fluctuations. Once the fluctuation-dissipation theorem does not hold for absorbing-state phase transitions, these quantities capture independent aspects of the transition. For example, while the standard mean-field exponents for short-ranged contact processes provides a divergent susceptibility at the critical point, it predicts $\gamma' = 0$, representing just a discontinuity in the order-parameter critical fluctuations.

According to the hyperscaling hypothesis, the values of the critical exponent ratio $\beta/\nu_\perp > 1/2$ reported to take place at low values of α point towards negative values of the exponent γ' governing the order-parameter fluctuations. This feature means that, in such regime, the order-parameter critical fluctuations vanish in the thermodynamic limit. In order to explicitly unveil this unconventional critical behavior, we computed the order-parameter fluctuations in the vicinity of the critical point. In Fig. 5 we report data from distinct system sizes for the same two representative values of the exponent α illustrated in the previous figures. Notice that for $\alpha = 3.0$ the order-parameter fluctuations develop a maximum at the critical point whose height grows with the system size [Fig. 5(a)], thus leading to the ultimate divergence of the critical fluctuations in the thermodynamic limit. On the other hand, the order-parameter fluctuations for $\alpha = 1.2$ [see Fig. 5(b)] do not show any diverging peak as the system size grows. Actually, the critical fluctuations indeed decrease with increasing system sizes [see inset in Fig. 5(b)]. In Fig. 6 we report the finite-size scaling behavior of the critical order-parameter fluctuations. The data consistently follow the power-law scaling predicted by the single length scale hypothesis. Therefore, the numerical simulation results corroborate the regime of vanishing order-parameter critical fluctuations anticipated by the hyperscaling relation. The set of values of the estimated exponent ratio $\gamma'/\nu_\perp$ is included in Table I. The independently estimated ratios $\beta/\nu_\perp$ and $\gamma'/\nu_\perp$ are in agreement with the hyperscaling relation within the estimated error bars [$(2\beta + \gamma')/\nu_\perp = d = 1$].

To further evidence the distinct critical behavior exhibited by the present model in the regimes of large and small values of α, we followed the relaxation dynamics towards the statistically stationary state. Starting from a configuration with all sites in the active state, the time evolution of the order parameter and its moment ratio and fluctuations can be used to estimate some dynamical critical exponents. In what follows, we considered the relaxation process in chains with $L = 2 \times 10^4$ sites and averaged the quantities over 10^4 distinct runs.

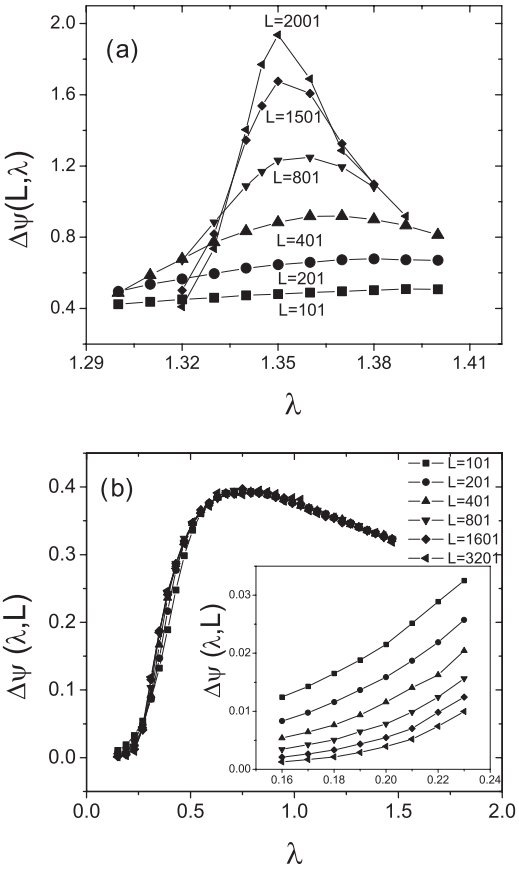

FIG. 5. Order-parameter density fluctuations for several lattice sizes as a function of the contamination rate λ in the vicinity of the critical point. The average was performed considering 10^4 distinct configurations taken at each L lattice sweeps. (a) $\alpha = 3.0$ showing growing critical fluctuations at the critical point as $L \to \infty$. (b) $\alpha = 1.2$, which does not show any increasing peak as the system size grows. Near the critical point (see the inset) the critical fluctuations decrease with increasing system sizes.

The order-parameter density relaxes towards its stationary value following the dynamic scaling law $\Psi(\lambda_c,t) \propto t^{-\beta/z\nu_\perp}$, where $z = \nu_\parallel/\nu_\perp$. In Fig. 7 we show such time evolution for distinct values of α. The ultimate saturation of the order-parameter density is a finite-size effect and results from the reflecting boundary condition used in our simulations. Notice that the relaxation becomes faster for small values of α. The estimated values of the exponent ratio $\beta/z\nu_\perp$ are reported in Table II. The dynamic scaling hypothesis also predicts that the moment ratio $m(\lambda_c,t) \propto t^{1/z}$. In Fig. 8 we report the relaxation of the order-parameter moment ratio. The estimated values of the dynamic exponent $1/z$ are also included in Table I. The increase of $1/z$ as $\alpha \to 1$ reflects the fast relaxation dynamics taking place in the regime of very long-ranged activation process. These two exponents can be used to obtain an independent estimate of the stationary exponent ratio $\beta/\nu_\perp$ and these agree with the values reported in Table I within the error bars. The here reported critical exponents are consistent with those reported in Ref. [30].

The time evolution of the order-parameter fluctuations is shown in Fig. 9. Dynamical scaling predicts $\Delta\Psi(\lambda_c,t) \propto t^{\gamma'/z\nu_\perp}$. Here one can see clearly the striking difference between

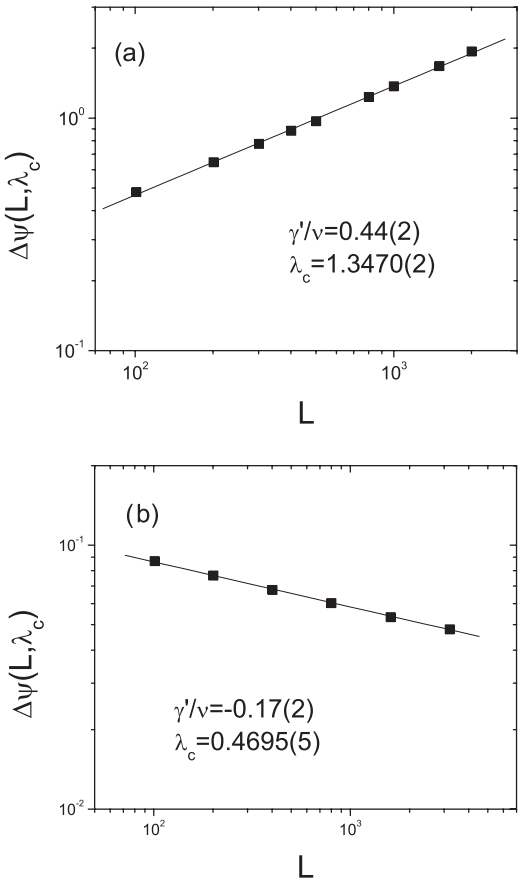

FIG. 6. Finite-size scaling of order-parameter fluctuations at the critical point. From the best fit to power laws, we estimate the corresponding critical exponent. (a) $\alpha = 3.0$ for which we estimate $\gamma'/\nu_\perp = 0.44(2)$. (b) $\alpha = 1.5$ for which we estimate $\gamma'/\nu_\perp = -0.17(2)$.

the regimes of short- and long-ranged interactions. The critical fluctuations grow in time for large values of α. As the activation process becomes longer ranged, i.e., as α decreases,

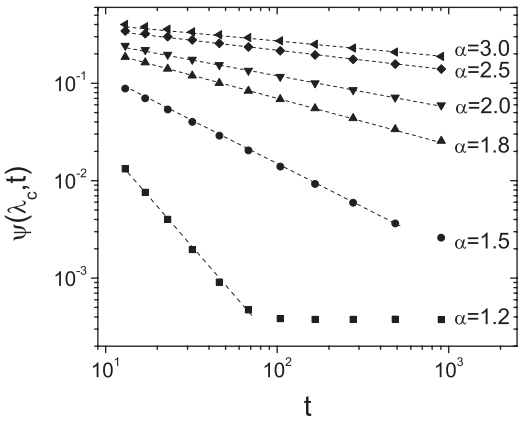

FIG. 7. Time evolution of the order parameter at the critical point for several values of α. The saturation at long times is a finite-size effect. Here we considered $L = 2 \times 10^4$ and averaged over 10^4 copies. Prior to saturation, the dynamic scaling law $\Psi(\lambda_c,t) \propto t^{-\beta/z\nu_\perp}$ holds. Estimates of this critical exponent ratio are reported in Table II.

TABLE II. Estimated dynamic critical exponents $\beta/z\nu_\perp$, $1/z$, and $\gamma'/z\nu_\perp$ for various values of the exponent α characterizing the long-distance infection process. We also include the critical infection rate λ_c as reported in Ref. [30]. In the regime on which $\gamma' < 0$ the critical order-parameter fluctuations decrease in time. $(2\beta + \gamma')/z\nu_\perp$ is also shown and, according to the hyperscaling relation, equals $1/z$.

α	λ_c	$\beta/z\nu_\perp$	$1/z$	$\gamma'/z\nu_\perp$	$(2\beta+\gamma')/z\nu_\perp$
1.2	0.205(3)	2.11(2)	2.81(6)	−1.41(3)	2.81(7)
1.5	0.4695(5)	0.88(2)	1.53(4)	−0.23(2)	1.53(6)
1.8	0.714(1)	0.46(2)	1.04(4)	0.12(2)	1.04(6)
2.0	0.8592(2)	0.32(2)	0.88(3)	0.22(1)	0.86(5)
2.5	1.1492(2)	0.20(1)	0.70(1)	0.30(1)	0.70(3)
3.0	1.3470(2)	0.17(1)	0.64(1)	0.31(1)	0.65(3)

a crossover to a regime of decreasing fluctuations sets up. The estimated critical exponent $\gamma'/z\nu_\perp$ are reported in Table II. All values of the reported exponents are in agreement with those estimated at the stationary state within the error bars. In Table II we also include the combined exponent $(2\beta + \gamma')/z\nu_\perp$ that, according to the hyperscaling relation, equals $1/z$. Again, the hyperscaling relation is satisfied within our present numerical accuracy.

Finally, to have a clearer picture of how the critical behavior changes as the activation process becomes longer ranged, we plot in Fig. 10 a set of representative space-time diagrams of the critical relaxation process. For large values of α, the critical activation ratio is relatively large because the activation mainly occurs through short-distance processes. This feature makes the time evolution slower and sustains a large number of active sites in the critical statistically stationary regime. On the other hand, a longer-ranged activation process (small values of α) requires a lower value of the critical activation ratio above which the active state can be sustained. Such a small value of the critical activation ratio thus implies in a faster relaxation. Further, as the activation process is frequently triggered by a long-distance process, a small number of active sites are required to sustain the critical active state, which results in

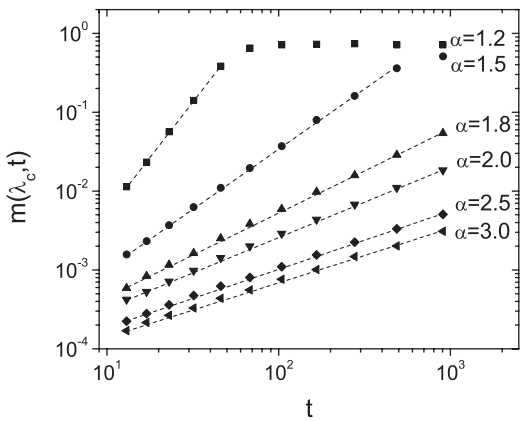

FIG. 8. Time evolution of the order-parameter moment ratio at the critical point for several values of α. The dynamic scaling law $m(\lambda_c,t) \propto t^{1/z}$ holds in the short time regime. Estimates of this critical exponent ratio are reported in Table II.

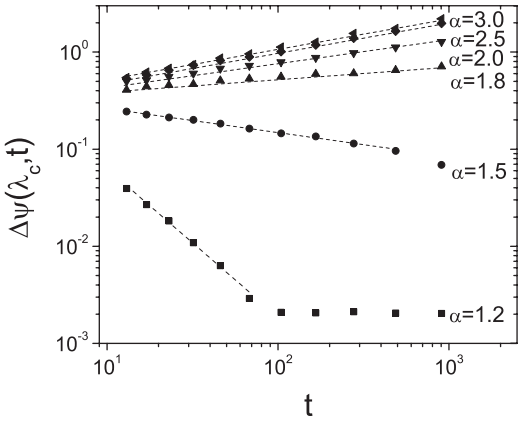

FIG. 9. Time evolution of the order-parameter fluctuations at the critical point for several values of α. The dynamic scaling law $\Delta\Psi(\lambda_c,t) \propto t^{\gamma'/z\nu_\perp}$ holds in the short time regime. Estimates of this critical exponent ratio are reported in Table II. Note that the critical fluctuations decrease in time for small values of α.

a sparser set of active sites at the critical stationary regime. Notice that, in the same range of values of the decay exponent α at which the critical fluctuations vanish, the order-parameter critical exponent β becomes larger than 1. This implies that the order-parameter derivative becomes continuous at the transition, being null both above and below the critical point. The above features are, ultimately, responsible for the vanishing of the order-parameter critical fluctuations in this regime.

IV. SUMMARY AND CONCLUSIONS

In summary, we provided an extensive scaling analysis of the critical behavior of the absorbing-state phase transition exhibited by a one-dimensional contact process model with long-distance activation introduced in Ref. [30]. The model considers that a given site can become active at a rate that decays as a power law of the distance to the nearest active site and presents an absorbing-state phase transition whose set of critical exponents continuously change as a function of the exponent α governing the decay of the activation process [30].

We explored the single length and time scales hypothesis to report a set of stationary and dynamical critical exponents for distinct regimes of the activation process. In particular, we explored the fact that the absence of detailed balance leading to the nonvalidity of the fluctuation dissipation theorem for absorbing-state phase transitions, together with the long-range character of the interactions, favors the emergence of a nonconventional second-order phase transition on which the order-parameter fluctuations vanish at criticality. We have numerically unveiled that such regime indeed sets up for small values of α, at which the critical exponent of the order-parameter fluctuations become negative. The space-time evolution of the relaxation process provided evidence for the key role played by the long-range process in this regime. In the presence of a long-range activation process, the critical activation rate is rather small and the critical relaxation process is faster than that taking place when only short-range interactions are relevant. In this scenario, a quite sparse active population is able to support the critical

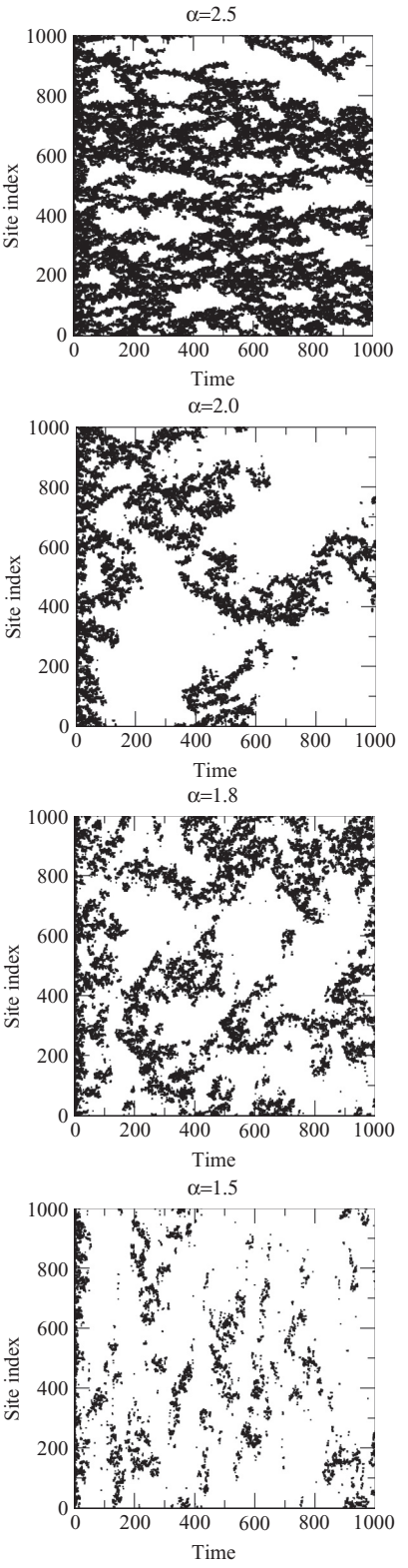

FIG. 10. Space-time diagrams of the relaxation process at the critical point for a set of representative values of α. For large values of α the activation process is mainly short ranged, thus leading to a slower critical relaxation and a denser active population at the critical stationary regime. On the other hand, the activation process is mainly long ranged for small values of α, resulting in a smaller critical activation rate, faster relaxation dynamics, and a sparser critical active population.

active state. In this sense, while equilibrium second-order transitions always present diverging critical fluctuations, a new class of nonequilibrium absorbing-state phase transitions with vanishing critical fluctuations is supported by systems with long-range interactions.

ACKNOWLEDGMENTS

We thank CAPES, CNPq, and FINEP (Brazilian Research Agencies) as well as FAPEAL (Alagoas State Research Agency) for partial financial support.

[1] H. B. Callen and T. A. Welton, Phys. Rev. **83**, 34 (1951).
[2] H. Hinrichsen, Adv. Phys. **49**, 815 (2000).
[3] G. Odor, Rev. Mod. Phys. **76**, 663 (2004)
[4] S. Lubeck, Int. J. Mod. Phys. B **18**, 3977 (2004).
[5] H. Hinrichsen, Physica A **369**, 1 (2006).
[6] J. Marro and R. Dickman, *Nonequilibrium Phase Transitions in Lattice Models* (Cambridge University Press, Cambridge, 1999).
[7] R. Dickman, in *Nonequilibrium Statistical Mechanics in One Dimension*, edited by Privman V. (Cambridge University Press, Cambridge, 1996).
[8] S. Lübeck and R. D. Willmann, Nucl. Phys. B **718**, 341 (2005).
[9] S. Lübeck and R. D. Willmann, J. Stat. Phys. **115**, 1231 (2004).
[10] T. M. Liggett, *Interacting Particle Systems* (Springer, Heidelberg, 1985).
[11] K. A. Takeuchi, M. Kuroda, H. Chaté, and M. Sano, Phys. Rev. Lett. **99**, 234503 (2007).
[12] K. A. Takeuchi, M. Kuroda, H. Chaté, and M. Sano, Phys. Rev. E **80**, 051116 (2009).
[13] J. Cardy and U. C. Tauber, Phys. Rev. Lett. **77**, 4780 (1996).
[14] I. Dornic, H. Chaté, J. Chave, and H. Hinrichsen, Phys. Rev. Lett. **87**, 045701 (2001).
[15] M. Rossi, R. Pastor-Satorras, and A. Vespignani, Phys. Rev. Lett. **85**, 1803 (2000).
[16] F. van Wijland, K. Oerding, and H. J. Hilhorst, Physica A **251**, 179 (1998).
[17] U. L. Fulco, D. N. Messias, and M. L. Lyra, Phys. Rev. E **63**, 066118 (2001).
[18] H. K. Janssen, Phys. Rev. E **64**, 058101 (2001).
[19] I. Dornic, H. Chaté, and M. A. Muñoz, Phys. Rev. Lett. **94**, 100601 (2005).
[20] M. M. de Oliveira and R. Dickman, Phys. Rev. E **74**, 011124 (2006).
[21] D. S. Maia and R. Dickman, J. Phys.: Condens. Matter **19**, 065143 (2007).
[22] N. V. da Costa, U. L. Fulco, M. L. Lyra, and I. M. Gleria, Phys. Rev. E **75**, 031112 (2007).
[23] R. Dickman and M. D. Souza, J. Phys. A **41**, 405002 (2008).
[24] C. Argolo, Yan Quintino, Y. Siqueira, Iram Gleria, and M. L. Lyra, Phys. Rev. E **80**, 061127 (2009).
[25] R. Dickman, L. T. Rolla, and V. Sidoravicius, J. Stat. Phys. **138**, 126 (2010).
[26] M. Henkel and H. Hinrichsen, J. Phys. A: Math. Gen. **37**, R117 (2004).
[27] M. C. Marques and A. L. Ferreira, J. Phys. A: Math. Gen. **27**, 3389 (1994).
[28] E. V. Albano, Europhys. Lett. **34**, 97 (1996).
[29] J. Adamek, M. Keller, A. Senftleben, and H. Hinrichsen, J. Stat. Mech. (2005) P09002.
[30] F. Ginelli, H. Hinrichsen, R. Livi, D. Mukamel, and A. Torcini, J. Stat. Mech. (2006) P08008.
[31] F. Ginelli, H. Hinrichsen, R. Livi, D. Mukamel, and A. Politi, Phys. Rev. E **71**, 026121 (2005).
[32] H. Hinrichsen, J. Stat. Mech. (2007) P07006.
[33] M. E. Fisher, S.-K. Ma, and B. G. Nickel, Phys. Rev. Lett. **29**, 917 (1972).
[34] E. Bayong, H. T. Diep, and Viktor Dotsenko, Phys. Rev. Lett. **83**, 14 (1999).
[35] E. Luijten and H. W. J. Blöte, Phys. Rev. Lett. **89**, 025703 (2002)
[36] S. S. Albuquerque, F. A. B. F. de Moura, M. L. Lyra, and A. J. F. de Souza, Phys. Rev. E **72**, 016116 (2005).
[37] R. Dickman and J. Kamphorst Leal da Silva, Phys. Rev. E **58**, 4266 (1998).